A stochastic 3D model based on random graphs to characterize the morphology of compact aggregates using image analysis

Léo Théodon, Carole Coufort-Saudejaud, Johan Debayle

A stochastic 3D model based on random graphs to characterize the morphology of compact aggregates using image analysis

Léo Théodon
CNRS, UMR 5307 LGF, Centre SPIN
MINES Saint-Etienne
Saint-Etienne, France
l.theodon@emse.fr

Carole Coufort-Saudejaud
Laboratoire de Génie Chimique
Université de Toulouse
CNRS, INPT, UPS, Toulouse, France
carole.saudejaud@toulouse-inp.fr

Johan Debayle
CNRS, UMR 5307 LGF, Centre SPIN
MINES Saint-Etienne
Saint-Etienne, France
debayle@emse.fr

***Abstract*—Morphological characterization of aggregates using image analysis is a key problem in many research areas. In particular, the estimation of 3D characteristics from projected 2D images is both complex and necessary. In this paper, a stochastic geometric 3D model called SWARM (Stochastic Wandering particle AgglomeRation Model) is developed based on hard sphere packing and random graphs. A method to adjust the model parameters by image analysis using morphological skeletons is presented and doubly validated on synthetic and 3D printed aggregates. The results obtained show relative errors of the order of 1% in most cases and 4% in the worst case, making it a very efficient model compared to similar models. Finally, limitations are discussed and possible improvements are suggested.**

***Index Terms*—Aggregates, Digital twins, Geometric modeling, Image analysis, Modeling, Simulation, Stochastic geometry**

I. Introduction

The morphological characterization of aggregates is critical in several industries, including pharmaceutical [1], food [2], chemical [3], and construction [4]. Their morphology influences their properties, affecting aspects such as taste [2], toxicity [1], environmental hazards, and mechanical strength [4]. Modeling these objects is essential, along with image analysis. Although image analysis typically provides limited two-dimensional data, when combined with a model, 3D morphological properties such as volume or surface area can be estimated under certain assumptions.

Morphological characterization of aggregates through image analysis is a dynamic research area [5], evolving with sophisticated image processing techniques [3, 6], model application [4], and recent advances in machine learning [1, 7–9]. However, when it comes to estimating 3D properties from a single 2D image, methods based on stochastic geometric models [10, 11] prove to be the most effective, the idea being to adjust the model parameters by matching the average 2D characteristics of the simulated objects with those measured on the images.

This paper develops a stochastic geometric model called SWARM (Stochastic Wandering particle AgglomeRation Model) based on hard spheres and random graphs. In the following section, the model is defined and examples of realizations are presented. The principle of fitting the parameters of the model to real data is then explained. The method is then validated twice, on synthetic aggregates and on 3D printed aggregates. Finally, limitations and perspectives are discussed. Table I shows the different morphological characteristics considered.

TABLE I: List of morphological characteristics.

Characteristic	Symbol	Definition and equation
Feret Diameter max.	F_{max}	Longest caliper (Feret) length
Feret Diameter min.	F_{min}	Smallest caliper (Feret) length
2D parameters		
Projected Area	A	Area of the object
Convex Area	A_c	Area of the convex hull
Perimeter	P	Length of the object outline
Aspect Ratio	AR	$F_{\text{min}}/F_{\text{max}}$
Convexity	Co	A/A_c
Circularity	C	$4\pi \times A/P^2$
3D parameters		
Volume	V	Volume of the object
Convex Volume	V_c	Volume of the convex hull
Surface Area	S	Area of the object surface
Equivalent Sphere Diameter	ESD	$2 \times \sqrt[3]{3 \times V/(4\pi)}$
Solidity	SLD	V/V_c
Sphericity	Φ_S	$6\pi^2 \times V/(\sqrt{\pi}S)^3$

II. The SWARM Model

The proposed SWARM model is based on the use of random graphs, which can be considered as the structure or skeleton of the aggregates to be generated. Consequently, it is necessary to define a procedure for generating random graphs with satisfactory properties, such as being fully connected. This article proposes the use of β-skeletons [12], using the definition of Neumann [13]. In the following section, the principle of generating a β-skeleton is explained in more detail. The SWARM model is then defined and examples of its implementation are shown.

A. Generating a β-skeleton

A β-skeleton is a graph whose number of edges depends indirectly on a parameter β. In fact, for each pair of vertices (p, q), an exclusion zone $R_{p,q}$ is defined whose size depends on β, and an edge e exists between these two vertices if and only if there is no other vertex in the exclusion zone.

The exclusion zone $R_{p,q}$ is defined as follows

$$R_{p,q} = \{x \in \mathbb{R}^3, \|x-m_1\| < \|q-m_1\| \wedge \|x-m_2\| < \|p-m_2\| \} \quad (1)$$

with

$$\begin{cases} m_1 = \frac{\beta}{2}p + \left(1 - \frac{\beta}{2}\right) q \\ m_2 = \frac{\beta}{2}q + \left(1 - \frac{\beta}{2}\right) p \end{cases} \quad (2)$$

Thus, the larger β, the larger the exclusion zone. In particular, with this definition and for $1 \leq \beta \leq 2$, the resulting graph is fully connected, with $\beta = 1$ being the Gabriel graph and $\beta = 2$ being the relative neighborhood graph. Furthermore, the computation of a beta skeleton with $\beta \geq 1$ is a subgraph of the Delaunay triangulation and can therefore be computed efficiently [14]. Fig. 1 illustrates the influence of the parameter β on the shape of the graph and the fact that it is fully connected for $1 \leq \beta \leq 2$.

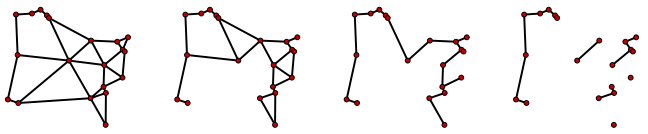

(a) $\beta = 1$ **(b)** $\beta = 1.5$ **(c)** $\beta = 2$ **(d)** $\beta = 3$

Fig. 1: Construction of a β-skeleton for the same set of vertices, with several different β values.

B. Model Definition

The SWARM model is based on an iterative process in which hard spheres are pulled by an attractive force toward a skeleton modeled by a random graph that determines the overall shape and form of the aggregate. The core algorithm of SWARM is the following:

1) A random graph $G = (P, E)$ is generated, where P is the set of vertices and E is the set of edges. If G is a β-skeleton, an easy-to-implement method is to generate P with a Poisson process of intensity λ and choose $\beta \in [1; 2]$.
2) The graph G is discretized and the gradient of the distance map to G is computed to obtain an attractive force field $\vec{g}$.
3) A number N_p of hard spheres are generated, randomly and uniformly distributed in $\mathbb{R}^3$. For each iteration, these spheres move according to the attractive force field $\vec{g}$ while maintaining a minimum distance from each other, depending on the overlap parameter d_α.

All the parameters required for the model are given in Table II, and Fig. 2 illustrates the process of generating an aggregate, from the construction of a random graph to the assembly of hard spheres. The number of iterations to run n_i is a semi-optional parameter in the sense that it avoids entering an infinite loop, since the stopping criterion is also triggered when the system is no longer evolving.

TABLE II: Listing of the SWARM model parameters.

Parameters	Definition
λ	Intensity of the Poisson point process
β	Control parameter for the random graph
N_p	Number of particles
r	Radius of the particles
d_α	Overlap parameter $\in [0; 1]$
$\Delta\rho$	Displacement step
n_i	Number of iterations to run

C. Example of Realizations

The SWARM model can be used to generate all kinds of compact aggregates (Fig. 3), whose morphology is primarily controlled by the underlying random graph. Thus, the morphological properties of the aggregates depend mainly on those of the random skeleton, primarily its shape, but also the edge density, which is controlled by the parameter β. Other properties, such as porosity, are controlled by the overlap parameter.

D. Performance

In terms of execution speed, the SWARM model developed in MATLAB® generates an aggregate with a number of particles $N_p = 400$ in a span of several tenths of a second on a computer equipped with an Intel® Core™ i9-12900KF processor at 3.19 GHz and 64GB of RAM. The factors that most significantly affect the execution speed of the model are the number of particles N_p, the number of iterations to run n_i

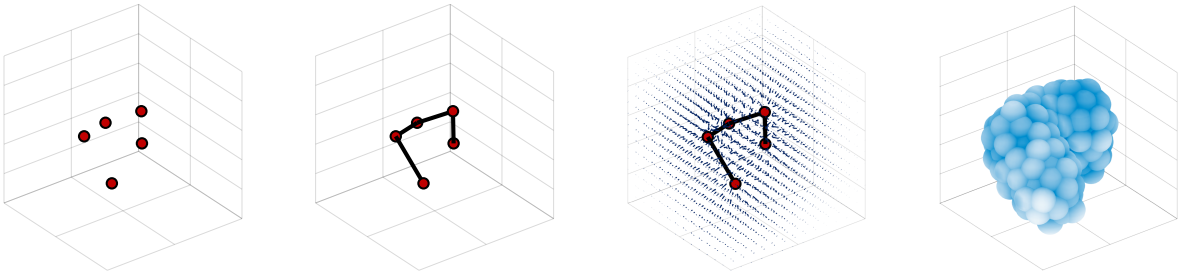

(a) Random points **(b)** β-skeleton **(c)** Attractive force field $\vec{g}$ **(d)** Final aggregate

Fig. 2: Aggregate generation process using the SWARM model.

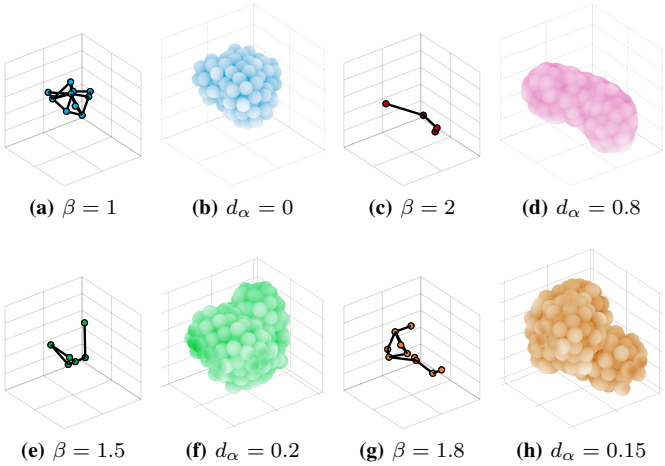

(a) $\beta = 1$ **(b)** $d_\alpha = 0$ **(c)** $\beta = 2$ **(d)** $d_\alpha = 0.8$

(e) $\beta = 1.5$ **(f)** $d_\alpha = 0.2$ **(g)** $\beta = 1.8$ **(h)** $d_\alpha = 0.15$

Fig. 3: Construction of a β-skeleton for the same set of vertices, with several different β values.

and the displacement step $\Delta\rho$, at the cost of a lower accuracy in the case of the latter.

These performances are intermediate between those of other stochastic geometric models based on hard spheres [10, 15]. However, the SWARM model has the significant advantage of being able to generate aggregates with complex geometry without assuming general convexity of the object shape.

III. Model Fitting

One of the main objectives of this paper is to demonstrate the ability of the SWARM model to infer the 3D morphological characteristics of an aggregate from a 2D image. This is achieved by adjusting the model parameters based on the information obtained by analyzing the 2D image.

In a very general framework, it would be appropriate to study an entire population of aggregates and deduce the optimal parameterization of the model, as well as the rules to be applied to the generation of random graphs (length, tortuosity, connectivity, etc.). However, the study of the rules governing the generation of random graphs is a complex problem that is beyond the scope of this article. Therefore, in the following, the graph used by the SWARM model to generate an aggregate will be derived directly from image analysis, allowing the optimization process to be applied only to the other 5 parameters of the model. However, it is necessary to assume that the studied aggregates have a globally *flat* geometry. The objects are therefore always observed along a preferred direction (orthogonal to the maximum Feret diameter), which is consistent with the way real images are captured by a morphogranulometer due to gravity. In the following sections, the method used to derive the graph to be used by the SWARM model from a 2D image is explained and the cost function chosen for the optimization process is defined.

A. Creating a Graph from a 2D Image

To illustrate the method for approximating the graph G to be used by the SWARM model as part of the optimization process for estimating 3D morphological properties from 2D images of aggregates, several synthetic aggregates have been generated using the SWARM model. 2D projections of these aggregates are generated and an approximation of the underlying graph is estimated by image analysis. This can be thought of as a kind of reverse engineering process.

The method can be broken down into three main steps.

1) The projected image is binarized and the morphological skeleton [16] is calculated and cleaned if necessary.
2) The skeleton is divided into sub-branches by computing endpoints and intersections. This step requires the use of Breadth-First Search type algorithms [17] to ensure that no branches are missed.
3) The non-parametric Ramer-Douglas-Peucker algorithm [18] is applied to each sub-branch to obtain a set of segments E. The final graph is $G = (P, E)$, where P is the set of endpoints and intersections of the morphological skeleton.

Fig. 4 illustrates these different steps. The SWARM model generates two aggregates (Fig. 4b and 4g) from two different graphs (Fig. 4a and 4f). Two 2D projections are made and binarized (Fig. 4c and 4h), the morphological skeleton is computed (Fig. 4d and 4i), and the graph approximation is estimated (Fig. 4e and 4j).

It clearly appears that the estimated graph is very close to the one used to generate the aggregates, and is therefore a good approximation that can be reintroduced as a parameter of the SWARM model. However, it must be emphasized that the developed method is only suitable for 2D graphs. Reconstruction and estimation of 3D graphs from 2D images is a complex problem [19] beyond the scope of this article. For this reason, the following section focuses on globally *flat* aggregates.

B. Cost Function Definition

To estimate the 3D characteristics of an aggregate from a 2D image projected using the SWARM model, it is necessary to apply the method for estimating the underlying G graph from the method described in the previous section, and then apply an optimization process to find the optimal

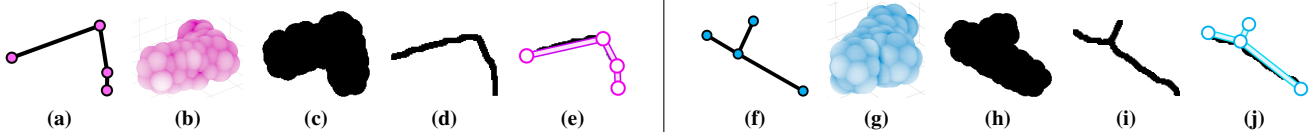

(a) **(b)** **(c)** **(d)** **(e)** **(f)** **(g)** **(h)** **(i)** **(j)**

Fig. 4: Illustration of the graph approximation method to be used by the SWARM model from a projected 2D image of an aggregate in two different cases.

values for the other 5 model parameters. This optimization process consists of minimizing a cost function $F_{\text{cost}}(\omega)$, where $\omega = \{N_p; r; d_\alpha; \Delta\rho; n_i\}$ is a parameterization of the SWARM model.

The cost function $F_{\text{cost}}(\omega)$ is defined as follows:

$$F_{\text{cost}}(\omega) = \Delta(A) + \Delta(P) + 2\Delta(\text{AR}) + \Delta(A_c) \qquad (3)$$

where A is the projected area, A_c is the convex area, P is the perimeter, and AR is the aspect ratio. $\Delta(x)$ is the relative error between the value of the characteristic x measured on the original 2D projected image and the average value proposed by the objects generated by the SWARM model.

The weights are determined empirically, after several trials, and the cost function $F_{\text{cost}}(\omega)$ is minimized by a genetic algorithm [20], since it is defined on a mixed product of continuous and discrete spaces, and this method has proven to be more efficient than simulated annealing [21], among others, in the context of this study.

In practice, the cost function $F_{\text{cost}}(\omega)$ is defined on a three-dimensional space. In fact, the number of iterations and the displacement step can be chosen to have no effect on the final result (the stopping criterion is a stable state of the system and the displacement step is sufficiently small). Although these choices may seem suboptimal, reducing the search space significantly speeds up the function optimization process.

IV. Model Validation

A. On Synthetic Data

An initial validation of the optimization process is carried out using the two synthetic aggregates generated by the SWARM model and presented in Fig. 4b and 4g. The idea is to ensure that it is possible, simply by relying on an analysis of the projected 2D images (Fig. 4c and 4h), to recover the initial parameterization of the model, as well as 3D characteristics close to those of the aggregates in Fig. 4.

For each of the two estimated graphs, an optimal set of parameters is obtained by optimizing the cost function $F_{\text{cost}}(\omega)$. Table III shows that these are very similar to the parameterizations used to generate the aggregates in Fig. 4b and 4g. Two sets of 400 aggregates are then generated for each of the optimal parameterizations, and their average morphological characteristics are compared with those of the original aggregates. Table IV shows the results obtained, with relative errors of no more than 3%, and in most cases less than 1%.

TABLE III: Comparison of the sets of parameters used to generate the synthetic 3D aggregates of Fig. 4 with the estimators returned by the optimization process.

(a) Fitting of Fig. 4b with $\widehat{\omega}_0$.

Parameters	N_p	r	d_α
Original values (ω_0)	120	0.70	0.50
Fitted values ($\widehat{\omega}_0$)	118	0.71	0.49
Error	1.7%	1.4%	2%

(b) Fitting of Fig. 4g with $\widehat{\omega}_1$.

Parameters	N_p	r	d_α
Original values (ω_1)	100	0.80	0.75
Fitted values ($\widehat{\omega}_1$)	101	0.78	0.74
Error	1.0%	2.5%	1.33%

Overall, the extremely low relative errors tend to validate the optimization method and process. In particular, it is possible to correctly estimate 3D morphological properties from the analysis of a 2D image. Finally, the causes of the discrepancies between the original values and the estimates are multifactorial.

- The graphs used for optimization are estimates of the original graphs.
- The optimal parameter sets are not exactly the same as the original sets.

In the next section, the method is further validated using 3D printed aggregates, demonstrating that the SWARM model is capable of simulating any type of compact aggregate.

B. On 3D Printed Aggregates

In this section, calibrated aggregates are 3D printed from a reference STL file representing a Blackberry (Fig. 5a). The printed aggregates are approximately 2mm long and 1.4mm wide and have a certain cylindrical symmetry, making them compatible with the image analysis method presented in the previous sections.

TABLE IV: Comparison of the average 2D and 3D morphological properties of 400 aggregates generated using optimal parameter sets $\widehat{\omega}_0$ and $\widehat{\omega}_1$ with those of the aggregates in Fig. 4b and 4g.

(a) Morphological characteristics with ω_0 vs. $\widehat{\omega}_0$

	2D						**3D**					
Characteristics	A (px^2)	A_c (px^2)	P (px)	AR	Co	C	V (px^3)	V_c (px^3)	S (px^2)	ESD (px)	SLD	Φ_S
Original Sample (ω_0)	13950	15851	513	0.76	0.88	0.66	43854	58651	7855	43.7	0.75	0.67
SWARM Fitting ($\widehat{\omega}_0$)	14057	15932	527	0.75	0.88	0.64	42615	56759	7745	43.5	0.75	0.66
Relative Error (%)	0.8%	0.5%	2.7%	1.3%	0%	3%	2.8%	3.2%	1.4%	0.5%	0%	0.7%

(b) Morphological characteristics with ω_1 vs. $\widehat{\omega}_1$

	2D						**3D**					
Characteristics	A (px^2)	A_c (px^2)	P (px)	AR	Co	C	V (px^3)	V_c (px^3)	S (px^2)	ESD (px)	SLD	Φ_S
Original Sample (ω_1)	13907	15388	511	0.6	0.90	0.67	43716	58651	7855	43.7	0.74	0.68
SWARM Fitting ($\widehat{\omega}_1$)	14057	15932	527	0.75	0.88	0.64	43761	58240	7812	43.7	0.75	0.67
Relative Error (%)	0.3%	0.8%	1.3%	3.3%	1.1%	3%	0.1%	0.7%	0.3%	0%	0.8%	0.3%

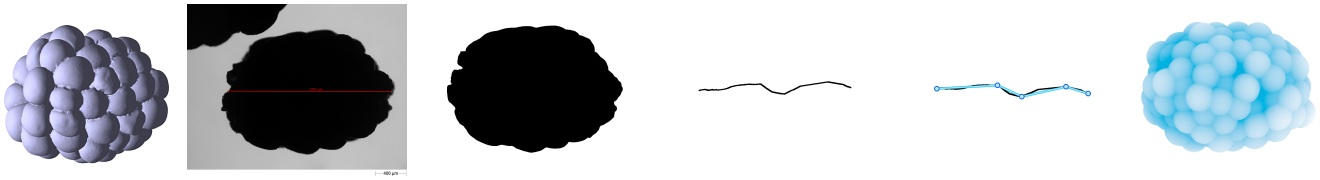

(a) STL file **(b)** 2D projection **(c)** Binary image **(d)** Skeleton **(e)** Estimated graph **(f)** Simulation

Fig. 5: Illustration of the process of generating real data by visualizing 3D printed aggregates using a morphogranulometer, image analysis to fit the SWARM model, and comparison with synthetic aggregates.

TABLE V: Comparison between 2D and 3D characteristics of 3D printed aggregates (ground truth) and synthetic aggregates generated by SWARM. The values shown for synthetic aggregates are averages calculated from a set of 400 aggregates.

	2D						**3D**					
Characteristics	A (mm^2)	A_c (mm^2)	P (mm)	AR	Co	C	V (mm^3)	V_c (mm^3)	S (mm^2)	ESD (mm)	SLD	Φ_S
Ground Truth	2.73	2.86	6.75	0.71	0.95	0.75	2.34	2.76	11.25	1.65	0.84	0.66
SWARM Model	2.72	2.85	6.82	0.72	0.95	0.74	2.34	2.74	11.94	1.65	0.85	0.68
Relative Error (%)	0.19%	0.15%	1.05%	0.92%	0.04%	2.25%	0.17%	0.76%	2.73%	0.06%	0.59%	4.06%

The 3D printed aggregates are analyzed using a morphogranulometer (Morphologi G3 – Malvern Panalytical). The resulting projected images (Fig. 5b) are then binarized (Fig. 5c) and an estimate of the underlying graph (Fig. 5e) is made from the morphological skeleton (Fig. 5d). After optimizing the parameters of the SWARM model, synthetic aggregates are generated (Fig. 5f) and their morphological characteristics are compared with those of the 3D printed aggregates.

Table V compares the morphological characteristics of the 3D printed aggregates – which are perfectly known thanks to the reference STL file, except for printing imperfections – with the average characteristics of a set of 400 aggregates simulated by the SWARM model after estimation of the underlying graph and parameter optimization. The results obtained are very satisfactory, with relative errors practically all below 1%, except for perimeter and area, which are always more difficult to calculate, and the characteristics that depend on them, without exceeding 4% relative error in the worst case. These larger errors in perimeter and surface area, which affect circularity and sphericity, may be due to the fact that the elementary particles used are hard spheres, whereas those in the 3D-printed aggregates are clearly not spherical.

C. Comparison with other methods

There are few methods for estimating 3D characteristics from a single 2D image. However, comparable methods recently developed, whether using hard sphere-based models [10, 15] or deforming a mesh with random fields [11], at best achieve results comparable to the SWARM model, and on the other hand are often more limited (symmetry assumptions, prior volume estimation, projection along a preferred direction, global convexity, etc.). On the other hand, the execution speed of the SWARM model, although significantly faster than models based on, for example, the Discrete Element Method, is in the low mid-range compared to these other stochastic geometric models.

V. Limitations & Prospects

Although the SWARM model is very flexible and capable of generating a large number of compact aggregates with complex geometries, it is not necessarily suitable for all situations and may have certain limitations.

- The method developed is particularly effective for aggregates with a globally flat geometry. On the other hand, for arbitrary aggregates, estimating the underlying graph from several 2D skeletons, for example, is a particularly complex problem.
- The SWARM model is not necessarily suitable for generating aggregates with low density and/or high porosity, such as soot particle aggregates.
- The method developed is limited to a single aggregate and cannot work in its current form for a population of aggregates.

However, a large number of approaches are still under investigation and will be the subject of future work. Some of the most promising prospects include the following.

- The method can be adapted to populations of aggregates by reducing the problem to estimating a population of random graphs. Once this population is correctly simulated, the process of optimizing the remaining parameters would be broadly similar. Moreover, by focusing on simulating a population of random graphs, it may no longer be necessary to assume that the geometry of the aggregates is globally flat.
- More prosaically, the method needs to be validated on a larger number of aggregates. 3D printed aggregates with more complex geometries would need to be created.
- As it stands, the method can still be adapted to a population of aggregates. It would then be necessary to repeat the process described in this article for a single aggregate as many times as necessary. Although tedious, it is not certain that this would be significantly slower than using Discrete Element Method models.

The main idea for future work is therefore to find a way to validate the method on a larger number of aggregates and to extend it to populations rather than single objects.

VI. Conclusion

A method based on the use of the SWARM model and the adjustment of its parameters using 2D image analysis techniques to estimate the 3D properties of aggregates has been developed and doubly validated, both numerically and using 3D printed aggregates. The two validations showed that the method is particularly suitable for compact aggregates with flat geometry, with relative errors on 2D and 3D morphological characteristics in the order of 1% in most cases and always below 4%, making it particularly competitive with other existing methods. Future work will aim to extend these results to populations of aggregates rather than individual objects.

Acknowledgment

The author(s) acknowledge(s) the support of the French Agence Nationale de la Recherche (ANR), under grant ANR-20-CE07-0025 (project MORPHING).

References

[1] A. Mehle, B. Likar, and D. Tomaževič, "In-line recognition of agglomerated pharmaceutical pellets with density-based clustering and convolutional neural network," in *2017 Fifteenth IAPR International Conference on Machine Vision Applications (MVA)*, 2017, pp. 9–12.

[2] I. Atalar and F. Yazici, "Effect of different binders on reconstitution behaviors and physical, structural, and morphological properties of fluidized bed agglomerated yoghurt powder," *Drying Technology*, vol. 37, no. 13, pp. 1656–1664, 2019.

[3] M. Pons, V. Plagnieux, H. Vivier, and D. Audet, "Comparison of methods for the characterisation by image analysis of crystalline agglomerates: The case of gibbsite," *Powder Technology*, vol. 157, no. 1, pp. 57–66, 2005.

[4] C. Jin, F. Zou, X. Yang, and Z. You, "3d quantification for aggregate morphology using surface discretization based on solid modeling," *Journal of Materials in Civil Engineering*, vol. 31, no. 7, p. 04019123, 2019.

[5] L. Théodon, J. Debayle, and C. Coufort-Saudejaud, "Morphological characterization of aggregates and agglomerates by image analysis: A systematic literature review," *Powder Technology*, vol. 430, p. 119033, 2023.

[6] N. Faria, M. Pons, S. Feyo de Azevedo, F. Rocha, and H. Vivier, "Quantification of the morphology of sucrose crystals by image analysis," *Powder Technology*, vol. 133, no. 1, pp. 54–67, 2003.

[7] M. Frei and F. E. Kruis, "Fully automated primary particle size analysis of agglomerates on transmission electron microscopy images via artificial neural networks," *Powder Technology*, vol. 332, pp. 120–130, 2018.

[8] P. Monchot, L. Coquelin, K. Guerroudj, N. Feltin, A. Delvallée, L. Crouzier, and N. Fischer, "Deep learning based instance segmentation of titanium dioxide particles in the form of agglomerates in scanning electron microscopy," *Nanomaterials*, vol. 11, no. 4, 2021.

[9] B. Rühle, J. F. Krumrey, and V.-D. Hodoroaba, "Workflow towards automated segmentation of agglomerated, non-spherical particles from electron microscopy images using artificial neural networks," *Scientific Reports*, vol. 11, no. 1, p. 4942, Mar. 2021.

[10] L. Théodon, C. Coufort-Saudejaud, and J. Debayle, "Grape: A stochastic geometrical 3d model for aggregates of particles with tunable 2d morphological projected properties," *Image Analysis & Stereology*, vol. 42, no. 1, pp. 1–16, 2023.

[11] ——, "A stochastic model based on gaussian random fields to characterize the morphology of granular objects," *Pattern Recognition*, vol. 149, p. 110255, 2024.

[12] J. Cardinal, S. Collette, and S. Langerman, "Empty region graphs," *Computational Geometry*, vol. 42, no. 3, pp. 183–195, 2009.

[13] M. Neumann, J. Staněk, O. M. Pecho, L. Holzer, V. Beneš, and V. Schmidt, "Stochastic 3d modeling of complex three-phase microstructures in sofc-electrodes with completely connected phases," *Computational Materials Science*, vol. 118, pp. 353–364, 2016.

[14] D. W. Matula and R. R. Sokal, "Properties of gabriel graphs relevant to geographic variation research and the clustering of points in the plane," *Geographical Analysis*, vol. 12, no. 3, pp. 205–222, 1980.

[15] L. Théodon, C. Coufort-Saudejaud, A. Hamieh, and J. Debayle, "Morphological characterization of compact aggregates using image analysis and a geometrical stochastic 3d model," in *2023 IEEE 13th International Conference on Pattern Recognition Systems (ICPRS)*, 2023, pp. 1–7.

[16] J. Serra, *Image Analysis and Mathematical Morphology*, ser. Image Analysis and Mathematical Morphology. Academic Press, 1982.

[17] S. S. Skiena, *Sorting and Searching*. London: Springer London, 2008, pp. 103–144.

[18] D. K. Prasad, M. K. Leung, C. Quek, and S.-Y. Cho, "A novel framework for making dominant point detection methods non-parametric," *Image and Vision Computing*, vol. 30, no. 11, pp. 843–859, 2012.

[19] S. Phon-Amnuaisuk, K. T. Murata, L.-O. Kovavisaruch, T.-H. Lim, P. Pavarangkoon, and T. Mizuhara, "Visual-based positioning and pose estimation," in *Neural Information Processing*, H. Yang, K. Pasupa, A. C.-S. Leung, J. T. Kwok, J. H. Chan, and I. King, Eds. Cham: Springer International Publishing, 2020, pp. 597–605.

[20] D. E. Goldberg, *Genetic Algorithms in Search, Optimization and Machine Learning*, 1st ed. USA: Addison-Wesley Longman Publishing Co., Inc., 1989.

[21] M. Pincus, "Letter to the editor—a monte carlo method for the approximate solution of certain types of constrained optimization problems," *Operations Research*, vol. 18, no. 6, pp. 1225–1228, 1970.